

Zonal necrosis prevented by transduction of the artificial anti-death FNK protein

S Asoh¹, T Mori², S Nagai¹, K Yamagata¹, K Nishimaki¹,
Y Miyato¹, Y Shidara^{1,3} and S Ohta^{*,1}

¹ Department of Biochemistry and Cell Biology, Institute of Development and Aging Sciences, Graduate School of Medicine, Nippon Medical School, Kawasaki-city, Kanagawa, Japan

² Saitama Medical Center/School, Kawagoe, Saitama, Japan

³ Department of Pathology, Tokyo Women's Medical University, School of Medicine, Shinjuku-ku, Tokyo, Japan

* Corresponding author: S Ohta, Department of Biochemistry and Cell Biology, Institute of Development and Aging Sciences, Graduate School of Medicine, Nippon Medical School, Kawasaki-city, Kanagawa 211-8533, Japan.
Tel: +81 44 733 9267; Fax: +81 44 733 9268; E-mail: ohta@nms.ac.jp

Received 28.6.04; revised 15.11.04; accepted 26.11.04; published online 04.2.05
Edited by H Ichijo

Abstract

Protection of cells from necrosis would be important for many medical applications. Here, we show protein transduction domain (PTD)-FNK therapeutics based on protein transduction to prevent necrosis and acute hepatic injury with zonal death induced by carbon tetrachloride (CCl₄). PTD-FNK is a fusion protein comprising the HIV/Tat PTD and FNK, a gain-of-function mutant of anti-apoptotic Bcl-x_L. PTD-FNK protected hepatoma HepG2 from necrotic death induced by CCl₄, and additionally, increased the apoptotic population among cells treated with CCl₄. A concomitant treatment with a pan-caspase inhibitor Z-VAD-FMK (N-benzyloxycarbonyl-Val-Ala-Asp-fluoromethylketone), which alone could not prevent the necrosis, protected these cells from the apoptosis. When pre-injected intraperitoneally, PTD-FNK markedly reduced zonal liver necrosis caused by CCl₄. Moreover, injection of PTD-FNK accompanied by Z-VAD-FMK suppressed necrotic injury even after CCl₄ administration. These results suggest that PTD-FNK has great potential for clinical applications to prevent cell death, whether from apoptosis or necrosis, and organ failure.

Cell Death and Differentiation (2005) 12, 384–394.

doi:10.1038/sj.cdd.4401569

Published online 4 February 2005

Keywords: necrosis; apoptosis; protein transduction domain; carbon tetrachloride; HepG2; liver; Bcl-x_L; protein therapeutics

Abbreviations: Ac-DEVD-AMC, *N*-acetyl-Asp-Glu-Val-Asp-7-amino-4-methylcoumarin; Ac-DEVD-CHO, *N*-acetyl-Asp-Glu-Val-Asp-CHO (aldehyde); ALT, alanine amino transferase; AST, aspartate amino transferase; CCl₄, carbon tetrachloride; DMEM, Dulbecco's modified Eagle's medium; ER, endoplasmic reticulum; *i.p.*, intraperitoneally; *s.c.*, subcutaneously; DEX, dexamethasone; TNF α , tumor necrosis factor α ; CHX, cycloheximide; PARP-1, poly(ADP-ribose) polymerase; PI, propidium iodide; PTD,

protein transduction domain; STS, staurosporine; Z-VAD-FMK, *N*-benzyloxycarbonyl-Val-Ala-Asp-fluoromethylketone; TUNEL, terminal deoxynucleotidyl transferase-mediated dUTP nick-end labeling

Introduction

Necrosis is morphologically distinct from apoptosis and defined as cell death accompanied by a rapid efflux of cell constituents to the extracellular space due to a loss of cytoplasmic membrane integrity.¹ Necrosis usually takes place under extremely harmful environmental conditions such as exposure to toxic chemicals, physical insults, and microbial pathogens and causes inflammation, which in turn gives rise to serious damage to surrounding cells.² Inflammatory responses can be controlled with anti-inflammatory agents, but necrosis itself cannot.^{3–5} Therefore, it is very important to reduce or prevent necrosis as a primary cause.

Anti-apoptotic proteins would provide novel means for therapeutic intervention to prevent massive cell death accompanying cell toxic injuries. In fact, a great number of studies have shown that anti-apoptotic members of the Bcl-2 family, Bcl-2 and Bcl-x_L, inhibit apoptosis of cultured cells induced by various death stimuli.^{6–11} On the other hand, a few *in vitro* studies^{12,13} showed that the proteins prevent necrotic cell death caused by a limited kind of death stimulus such as hyposia, where necrosis coexists with apoptosis. In these cases, necrosis appeared to be initiated by apoptosis-inducing reagents, and then ATP depletion resulted in a necrotic morphology. Thus, the anti-apoptotic proteins seem to exhibit anti-cell death activity against some forms of necrosis, which involve apoptotic machinery to some extent.

FNK (originally designated Bcl-xFNK in Asoh *et al.*¹⁴) was constructed from Bcl-x_L by the site-directed mutagenesis of three amino acids (Y22F/ Q26N/ R165K) to strengthen cytoprotective activity. FNK is the sole mutant with a gain-of-function phenotype among the mammalian anti-apoptotic factors, as FNK exhibited the stronger anti-apoptotic activity than Bcl-x_L to protect cultured cells from death induced by various death stimuli including oxidative stress, a calcium ionophore (A23187) and withdrawal of growth factors.¹⁴ It has been shown that proteins are directly and readily introduced into cells regardless of their molecular size when fused with the PTD (protein transduction domain) of HIV/Tat protein.¹⁵ PTD-fused proteins can be delivered to several tissues, including the brain, when injected into mice systemically.¹⁶ In addition, PTD-FNK, a fusion protein of the PTD and FNK, penetrates the dense matrix of cartilage to reach chondrocytes.¹⁷ In a previous study, PTD-FNK was demonstrated to reduce ischemic injury to hippocampal CA1 neurons after a transient forebrain ischemia,¹⁸ which involves slow progressive neuronal degeneration, and an apoptotic pathway is suggested to contribute to the ischemic degeneration, to some extent.¹⁹

The enhanced cytoprotective activity of FNK against oxidative stress and a calcium ionophore give rise to the possibility that FNK effectively protects cells from necrosis as well as apoptosis, because oxidative stress^{20–22} and a disruption of calcium homeostasis^{23–25} are known to induce necrosis. Carbon tetrachloride (CCl₄) has been used to induce necrosis in control experiments for studies on apoptosis^{26–29} and is one of most typical model agents for studying the pathogenesis of liver injury. The hepatotoxicity of CCl₄ *in vivo* has been well studied, indicating the importance of the reductive dehalogenation of CCl₄ catalyzed by cytochrome P450 in the endoplasmic reticulum (ER) as the initial event of the toxic cascades,^{30–34} and it is widely accepted that CCl₄ causes hepatic centrilobular necrosis.

Here, we show that the treatment of mice with PTD-FNK mitigated liver injury, including zonal necrosis, induced by CCl₄.

Results

Necrosis in HepG2 induced by CCl₄

We used a cell line HepG2 derived from hepatocyte cells as in *in vitro* experiments. HepG2 started to die in Dulbecco's modified Eagle's medium (DMEM) containing 80% saturation of CCl₄ in the absence of serum at 4 h and the survival rate at 8 h was 5.5% (Figure 1a). Thus, the CCl₄-induced death is not due to an immediate damage by CCl₄ as reported.³⁵ Nuclear staining with propidium iodide (PI)/Hoechst 33342 showed that PI-positive cells increased in number with time and that a majority of dead cells had a round nucleus uniformly stained with PI (Figure 1e). Their nuclear morphology is different from that of the cells killed by staurosporine (STS), which clearly caused nuclear fragmentation, one of the typical features of apoptosis (Figure 2c, top left panel). To characterize biochemically the death form of HepG2 cells treated with CCl₄, caspase-3/caspase-3-like activity, DNA fragmentation (laddering) and cleavage pattern of poly(ADP-ribose) polymerase-1 (PARP-1) were compared among the cells treated with CCl₄, STS and tumor necrosis factor α (TNF α). STS induced caspase-3-like activity at 4 h, with a plateau reached at 6 h, but CCl₄ had no effect even at 8 h (Figure 1b). DNA fragmentation was detected at 6 h and clearly observed at 8 h in STS-treated, but not CCl₄-treated cells (Figure 1c). TNF α with cycloheximide (CHX) is known to induce apoptosis in HepG2.^{36,37} PARP-1, a target of caspase-3, was cleaved into apoptotic fragments including the 85 kDa polypeptide in cells treated with TNF α /CHX (Figure 1d, indicated by an asterisk). In contrast, a fragment of 50 kDa, derived from PARP-1, clearly appeared in the CCl₄-treated cells at 4 h and decreased at 8 h (Figure 1d, indicated by an arrow). The 50 kDa fragment was designated as a major necrotic fragment.^{38–40} From these results, we confirmed that the death of HepG2 cells induced by CCl₄ is predominantly due to necrosis.

Protection of HepG2 from TNF α /CHX-induced apoptotic death by FNK transduction

PTD-FNK was shown to readily enter cultured cells of a neuroblastoma, SH-SY5Y, in 30 min to 1 h in a previous

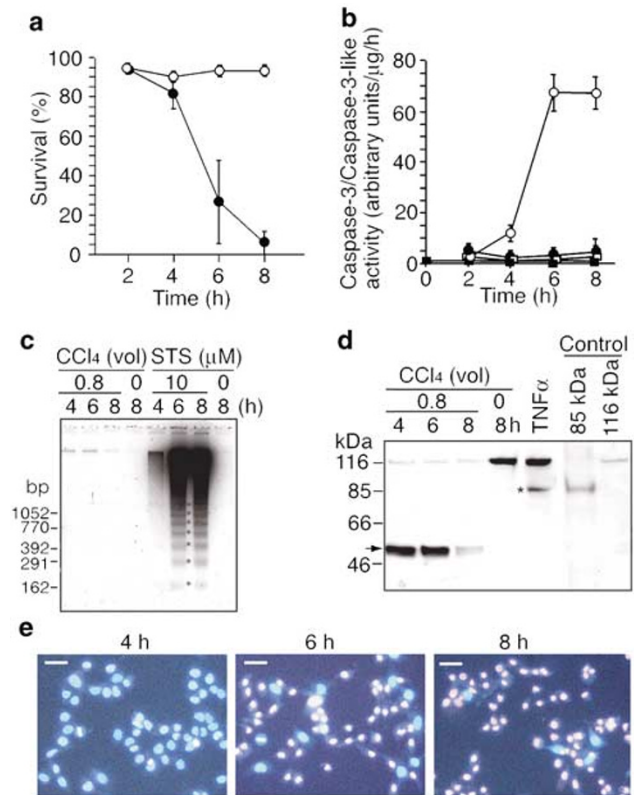


Figure 1 CCl₄ induces necrotic death of HepG2. (a) Cells were incubated with DMEM lacking FBS in the presence (closed circle) or absence (open circle) of 80%-saturated CCl₄ for the indicated time periods. The cells were stained with Hoechst 33342 and PI to calculate survival (%); 100 × (Hoechst-stained cells / (Hoechst-stained cells + PI-stained cells)). The mean of four independent wells (four fields of view per well) is shown with the S.D. (vertical bars). (b) Cells were incubated with the complete medium in the presence (open circle) or absence (closed circle) of STS, or with DMEM lacking FBS in the presence (open square) or absence (closed square) of 80%-saturated CCl₄ for the indicated time periods. The cells were harvested to prepare cell lysates for the caspase-3/caspase-3-like activity assay. The enzyme activity (mean with S.D.) is shown as arbitrary units/mg protein/h. (c) Cells were treated with CCl₄ or STS as described in (b). The harvested cells were treated with Triton X-100, and then centrifuged to remove intact nuclei. After propanol precipitation, fragmented DNAs were subjected to agarose gel electrophoresis. The STS-treated cells (8 h) showed a clear DNA ladder (marked with stars). (d) Western blot analysis of PARP. Total proteins were prepared from cells treated with CCl₄ for 4, 6 and 8 h, cells treated with DMEM for 8 h and cells treated with TNF α (10 ng/ml) and CHX (10 μg/ml) for 7 h, as described in Materials and methods. The total protein (30 μg) was subjected to Western blot analysis using an anti-body against PARP. Jurkat control lysate (BD Biosciences Pharmingen) and HL-60 cell extract (induced by etoposide) (Calbiochem), were also used for controls of the 116 kDa intact and the 85 kDa fragment of human PARP, respectively. The 85 kDa fragment appeared in the cells treated with TNF α (marked with*). An arrow indicates a 50 kDa fragment derived from PARP. (e) Representative images of cells incubated with DMEM lacking FBS in the presence of 80%-saturated CCl₄ for the indicated time periods. The cells were stained with Hoechst 33342 and PI. Scale bars: 50 μm

study.¹⁸ A pleiotropic cytokine, TNF α , has been shown to induce apoptosis and be involved in acute CCl₄-induced hepatic injury.^{41–43} We investigated whether PTD-FNK prevents HepG2 from TNF α /CHX-induced apoptosis. Cells were pretreated with PTD-FNK and incubated with TNF α /CHX in the presence of PTD-FNK. PTD-FNK significantly protected HepG2 against the cytotoxicity of TNF α (Figure 2).

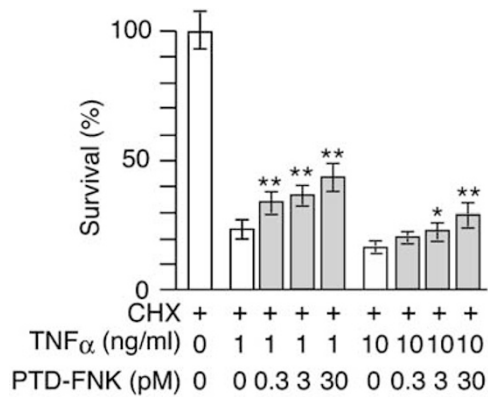


Figure 2 PTD-FNK protects HepG2 against TNF α -induced apoptosis. Cells were washed with FBS-free DMEM, and treated with various concentrations of PTD-FNK in FBS-free DMEM for 1 h, followed by incubation with DMEM containing FBS (10%) and CHX (10 μ g/ml) for 30 min. The cells were cultured with TNF α (1 or 10 ng/ml) for 12 h, and cells surviving were enumerated under a microscope by the trypan blue exclusion method. Means of three independent wells are shown with the S.D. Statistical analysis was performed using one-way ANOVA: *, $P < 0.05$; **, $P < 0.01$, versus control

Protection of HepG2 from CCl₄-induced necrotic death by FNK transduction

Next, to examine the cytoprotective effect of PTD-FNK on CCl₄-induced cell death in HepG2, PTD-FNK-pretreated cells were incubated with CCl₄ in the presence of PTD-FNK. Survival rates of the cells treated with PTD-FNK significantly increased up to 3 nM in a concentration-dependent manner and slightly decreased at the higher concentrations (Figure 3a (open bars) and c), indicating that PTD-FNK alone suppresses cell death induced by CCl₄. Comparison of the cytoprotective activity between PTD-FNK and PTD-Bcl-x_L showed that the activity of the former is stronger (Figure 3a and c).

Conversion of necrotic features into apoptotic ones forced by PTD-FNK

During this experiment, we noticed that a substantial population of dying cells treated with PTD-FNK had fragmented nuclei whose morphology was observed when treated with STS (Figure 3c, arrowheads and insets). The population of dead cell carrying a fragmented nucleus increased with the concentration of PTD-FNK, varying from 2.0 to 10% among cells with PTD-FNK treatment (Figure 3a, gray bars).

To confirm whether the dead cells with fragmented nuclei underwent apoptosis, HepG2 cells were exposed to CCl₄ in the presence of Z-VAD-FMK, a cell-permeable pan-caspase inhibitor. Z-VAD-FMK fully inhibited the STS-induced apoptosis of HepG2 (Figure 3c, leftmost panels). Importantly, the survival rate of cells co-treated with PTD-FNK and Z-VAD-FMK was significantly higher than that of cells treated with Z-VAD-FMK alone (Figure 3b). More interestingly, much more of the cells treated with a combination of PTD-FNK or PTD-Bcl-x_L and Z-VAD-FMK were survived than the cells treated with PTD-FNK or PTD-Bcl-x_L alone, and the combination treatment significantly decreased the number of dying cells

carrying fragmented nuclei (Figure 3b). These findings strongly suggest that PTD-FNK can protect a majority of HepG2 cells from necrotic death caused by CCl₄, and that PTD-FNK forced the cells in a necrotic pathway into an apoptotic pathway and then Z-VAD-FMK inhibited cell death in the apoptotic pathway.

Furthermore, we tried to detect an early stage of apoptosis by examining the binding of Annexin V to the surface of cells. Cells were exposed to CCl₄ in the absence or presence of PTD-FNK. Some cells were clearly stained with Annexin-V-FLUOS but not with PI (Figure 3e, arrowheads in the lower middle panel). Such Annexin-V-positive and PI-negative cells markedly increased depending upon the addition of PTD-FNK (Figure 3d). In contrast, the Annexin-V-positive and PI-negative population among the cells treated only with CCl₄ was very low and equivalent with that among the cells untreated with CCl₄ (Figure 3d), suggesting that the small population of apoptotic cells was due to the depletion of serum but not by the exposure to CCl₄. Taken together, these results strongly suggest that PTD-FNK leads cells to an apoptotic pathway from the necrotic process induced by CCl₄.

PTD-FNK retains the mitochondrial membrane potential and intracellular ATP level

After entering cells, PTD-FNK localizes to mitochondria.^{17,18} We examined the levels of intracellular ATP and the mitochondrial membrane potential to reveal the role of PTD-FNK on mitochondrial functions during the protection against necrosis. Exposure against CCl₄ decreased the intracellular ATP and PTD-FNK slightly but significantly suppressed the decrease (Figure 4a). Then, we examined the mitochondria membrane potential in CCl₄-treated cells in the presence or absence of PTD-FNK at 4 h, using mitochondria-specific fluorescent dyes, MitoTracker Red CMXRos and MitoTracker Green FM. MitoTracker Red stains mitochondria, depending upon the membrane potential, while MitoTracker Green FM depends upon the mitochondrial mass in a membrane potential-independent manner. Thus, the relative mitochondrial potential level was estimated by normalizing the red fluorescence with the green one. CCl₄ decreased the membrane potential to 68% of the initial level, and PTD-FNK completely inhibited the decrease (Figure 4b). It is noted that pre-incubation with PTD-FNK did not affect the intracellular ATP levels and the mitochondria membrane potential (Figure 4a and b at 0 time).

Delivery of PTD-FNK into the liver

The tissue delivery of the fused protein, PTD-FNK, injected intraperitoneally (*i.p.*) into 7-week-old male mice was examined by immunohistochemical staining. At 12 h after the injection, exogenous PTD-FNK was detected in the liver by using monoclonal anti-Bcl-x antibody, which recognizes the FNK protein as well as Bcl-x_L (Figure 5a). The protein appeared to be distributed ubiquitously. Next, we tested the delivery of the PTD-FNK protein into liver by injecting subcutaneously (*s.c.*) PTD-FNK. At 1, 3, 5 and 12 h after injection, livers were removed for staining with the monoclonal

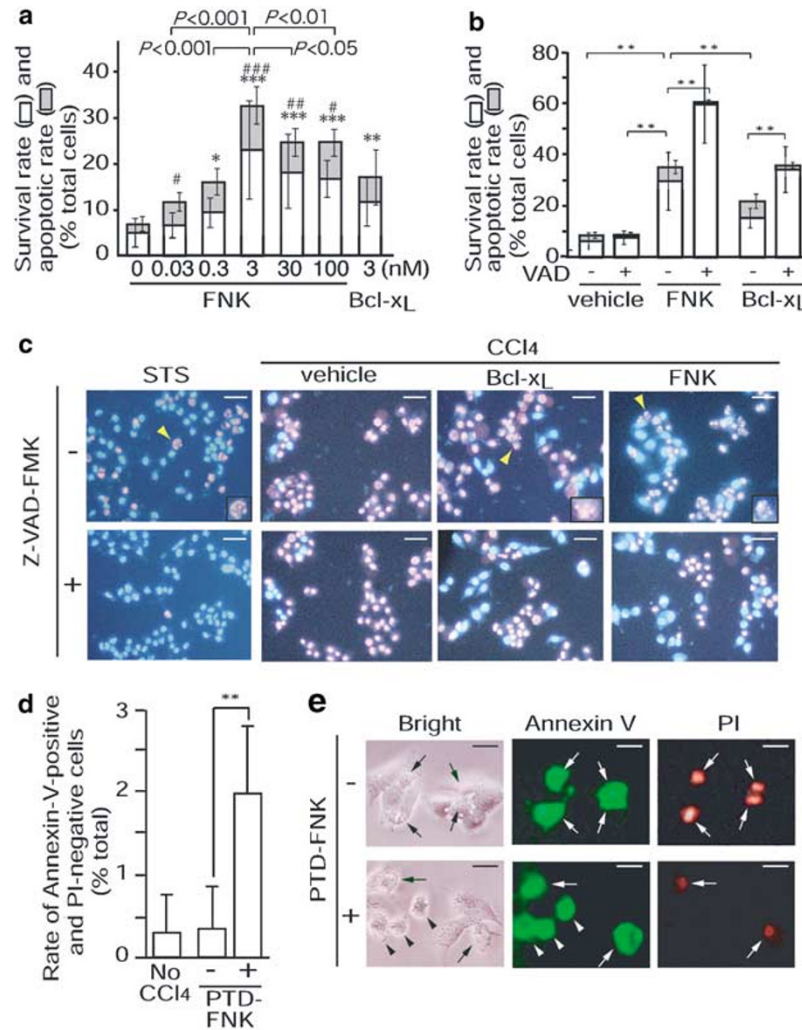


Figure 3 PT-D-FNK prevents necrotic death of HepG2. (a) Cells were incubated with PT-D-FNK (FNK) or PT-D-Bcl-xL (Bcl-xL) at the indicated concentrations in FBS-free DMEM for 1 h, after washed with FBS-free DMEM. The cells were then treated with 80%-saturated CCl₄ for 8 h in the presence of PT-D-FNK (FNK) or PT-D-Bcl-xL (Bcl-xL) at the indicated concentrations. The cells were stained with Hoechst 33342 and PI to calculate the survival rate (open bar) and apoptotic rate (PI-stained cells with a fragmented nucleus; gray bar) as described in Figure 1a. The mean of four independent wells (four fields of view per well) is shown with the S.D. (vertical bars). Statistical analysis was performed for the survival rate by one-way ANOVA. *, $P < 0.05$; **, $P < 0.01$; ***, $P < 0.001$, compared with FNK 0 nM; #, $P < 0.05$; ##, $P < 0.01$; ###, $P < 0.001$, compared with Bcl-xL 3 nM. (b) Cells were pre-incubated with vehicle, 3 nM PT-D-FNK (FNK) or 3 nM PT-D-Bcl-xL (Bcl-xL) in FBS-free DMEM in the presence or absence of Z-VAD-FMK (VAD, 50 μ M) for 1 h, after washed with FBS-free DMEM. The cells were then treated with 80%-saturated CCl₄ for 8 h in the presence or absence of 3 nM PT-D-FNK (FNK), 3 nM PT-D-Bcl-xL (Bcl-xL) or 50 μ M Z-VAD-FMK as indicated. The cells were stained with Hoechst 33342 and PI to calculate the survival rate (open bar) and apoptotic rate (gray bar) as described in Figure 2a. The mean of four independent wells (four fields of view per well) is shown with the S.D. (vertical bars). Statistical analysis was performed for the survival rate using one-way ANOVA: *, $P < 0.05$; **, $P < 0.001$. (c) Representative images of cells described in Figure 2b and cells treated with STS (10 μ M) in the presence or absence of Z-VAD-FMK (50 μ M) for 12 h. For the cells treated with STS and Z-VAD-FMK, Z-VAD-FMK was added 1 h before the STS treatment. PI-stained cells with a fragmented nucleus are shown by arrowheads and enlarged (insets). Scale bars: 50 μ m. (d) Cells were pre-incubated with 3 nM PT-D-FNK (+) or vehicle (-) in FBS-free DMEM for 1 h, after washed with FBS-free DMEM. The cells pre-treated with PT-D-FNK or vehicle were incubated with 80%-saturated CCl₄ containing 3 nM PT-D-FNK or vehicle, respectively, for 3 h. Cells without any pre-treatment were also incubated with DMEM lacking FBS (no CCl₄) for 3 h. The cells were stained with Annexin-V-FLUOS and PI to calculate the rate of Annexin-V-positive and PI-negative cells (%); 100 \times Annexin-V-positive and PI-negative cells/total cells in a bright field of view. The mean of three independent wells (three to four fields of view per well) is shown with the S.D. (vertical bars). **, $P < 0.0001$ by the Student's *t*-test. (e) Representative images of cells described in Figure 2d are shown. Bright, bright field; Annexin V, Annexin-V-FLUOS staining (green); PI, PI staining (red); arrowheads, apoptotic cells; arrows, necrotic or dead cells. Scale bars: 25 μ m

anti-Bcl-x antibody. Immunoreactivity was found in the centrilobular region at 1 h and extensive intracellular accumulation of PT-D-FNK was observed at 3 h (Figure 5b). The reactivity peaked at 3 h after injection and gradually decreased but clearly remained until 12 h, compared with vehicle injection (Figure 5b and c). Thus, these results indicate that PT-D-FNK is promptly delivered to liver by *s.c.* injection as well as *i.p.* administration.

Pre-treatment with PT-D-FNK prevents acute liver injury induced by CCl₄

To assess the activity of FNK delivered into the liver to inhibit acute and chronic CCl₄-induced injuries, mice injected with the PT-D-FNK protein were treated with CCl₄. Injection of CCl₄ caused a variety of toxic changes such as zonal necrosis, hydropic degeneration of cytoplasm or pyknosis/loss of

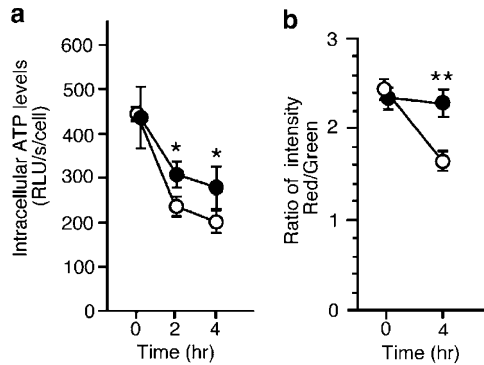


Figure 4 PTD-FNK retains the levels of cellular ATP and the mitochondrial membrane potential in the presence of CCl_4 . **(a)** Cells were pre-incubated with 3 nM PTD-FNK (closed circle) or vehicle (open circle) in FBS-free DMEM for 1 h, and continued to culture with 80%-saturated CCl_4 containing 3 nM PTD-FNK or vehicle for the periods indicated. The level of Intracellular ATP per cell was determined using luminescence as described in Materials and methods. Mean values of three independent wells are shown with the S.D. (vertical bars). Statistical analysis was performed using one-way ANOVA: *, $P < 0.05$, compared with vehicle. **(b)** Cells were pre-incubated with 3 nM PTD-FNK (closed circle) or vehicle (open circle) in FBS-free DMEM for 1 h and cultured with 80%-saturated CCl_4 in the presence of 3 nM PTD-FNK or vehicle for the periods indicated, followed by being stained with MitoTracker Red and MitoTracker Green FM in fresh DMEM for 30 min. The intensity of fluorescence from each cell was imaged by confocal scanning laser microscopy, and analyzed by using the NIH IMAGE program. Values are expressed as a ratio of the intensity in red divided by that in green of each cell. The mean of the cells examined (PTD-FNK at time 0 and 4 h, 415 and 442 cells, respectively; vehicle at time 0 and 4 h, 425 and 372 cells, respectively) is shown with the S.E. (vertical bars). Statistical analysis was performed using one-way ANOVA: **, $P < 0.001$, compared with a vehicle control

nucleus in hepatic cells at both acute and chronic phases (Figures 6c and 7b). A pathologist blindly performed the semi-quantitative histopathological analysis (Table 1).

Pre-injection of PTD-FNK (300 $\mu\text{g}/\text{kg}$) markedly ameliorated this zonal necrosis (Figure 6d and Table 1). Hydropic degeneration of the cytoplasm and pyknosis or loss of nuclei were observed to a small extent in the hepatic cells of mice injected with PTD-FNK, compared to control mice. Serum transaminases, releasing enzymes alanine amino transferase (ALT) and aspartate amino transferase (AST), were measured to evaluate the severity of acute liver injury as a whole (Figure 6a and b). PTD-FNK (300 $\mu\text{g}/\text{kg}$) markedly decreased both activities by two-thirds, compared to vehicle injection. The lower dose of PTD-FNK (75 $\mu\text{g}/\text{kg}$) suppressed the release from liver by one-third compared with the vehicle injection, although the effect was statistically insignificant. The ALT activity decreased at day 2 and was close to a normal level (Figure 7a) on day 3 (data not shown). PTD-Bcl- x_L (300 $\mu\text{g}/\text{kg}$) did not exhibit activity to suppress the release of the enzymes, indicating that PTD-FNK has the stronger activity to protect hepatocytes from cell death induced by CCl_4 *in vivo* as well as *in vitro*.

Post-treatment with PTD-FNK improves acute hepatic injury with a caspase inhibitor

Post-injection of PTD-FNK seemed to only slightly reduce ALT and AST activities in serum (Figure 6a and b), although

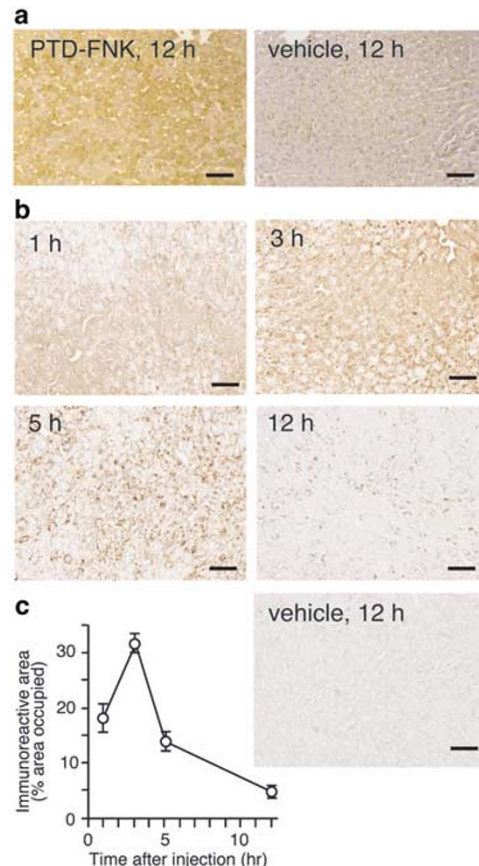


Figure 5 The PTD-FNK protein can be transduced into liver. Male mice (7 weeks old) were injected *i.p.* or *s.c.* with vehicle or PTD-FNK (50 mg/kg). After the indicated periods, the mice were transcardially perfused with cold heparinized physiological saline followed by 4% paraformaldehyde in phosphate-buffered saline (PBS, 0.1 M, pH 7.4), dehydrated and embedded in paraffin. Sections of liver were prepared and subjected to immunohistochemical staining (brown) using anti rat Bcl-x serum. **(a)** *I.p.* injection of PTD-FNK (left) and vehicle (right). Livers were removed at 12 h after *i.p.* These sections were counterstained with hematoxylin (purple) after immunohistochemical staining. Scale bars: 50 μm . **(b)** *S.c.* injection of PTD-FNK. Livers were removed at 1, 3, 5 and 12 h after *s.c.* injection. The immunostained image of liver removed at 12 h after *s.c.* injection of vehicle is also shown. Scale bars: 50 μm . **(c)** Quantitative evaluation of the PTD-FNK remaining in liver after *s.c.* injection. Low-magnification digital images (a half-magnification of (b)) of five fields in liver at each time point were analyzed to determine relative areas occupied by Bcl-x immunoreactivity with NIH IMAGE software. The value for liver sections of mice injected with vehicle was used as a background to be subtracted from that for mice injected with the protein. After statistical analysis by one-way ANOVA, the data are shown as means with S.D. (vertical bars). Following the peak at 3 h, PTD-FNK in the liver tissue decreased with a half-span of 3.5 h

zonal necrosis was apparently inhibited (Figure 6e and Table 1). The *in vitro* results described above led us to post-inject PTD-FNK with Z-VAD-FMK. The combined post-injection significantly suppressed the elevation of serum ALT and AST, while injection of Z-VAD-FMK alone did not (Figure 6a and b). Histopathological examination also showed that the combined injection profoundly inhibited zonal necrosis (Figure 6f and Table 1). However, no typical apoptotic hepatocyte was found by the TUNEL assay regardless of the injection of PTD-FNK (data not shown).

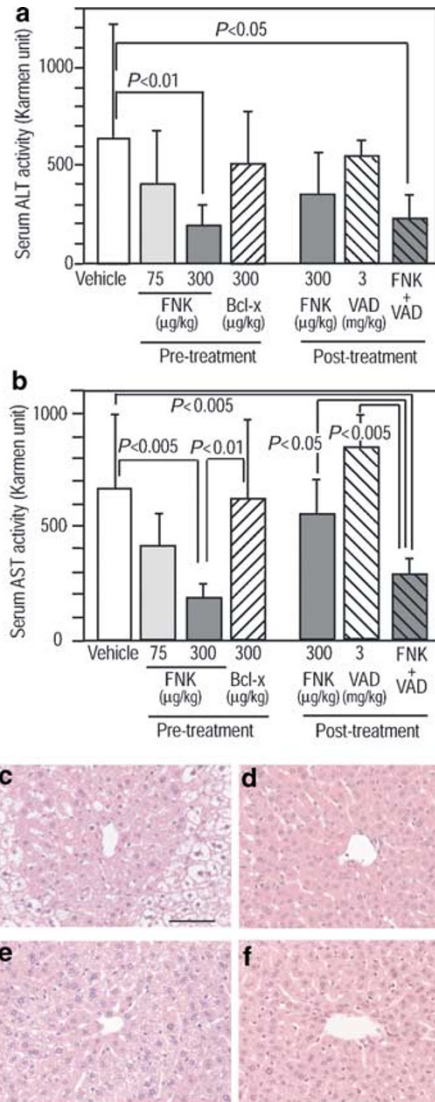


Figure 6 PTD-FNK prevents acute liver injury caused by CCl_4 . (a and b) Animals were *i.p.* injected with vehicle ($n=6$), PTD-FNK (FNK; 75 $\mu\text{g/kg}$, $n=5$; 300 $\mu\text{g/kg}$, $n=6$) or PTD-Bcl- x_L (Bcl- x_L ; $n=6$) 3 h before the administration of CCl_4 (pre-treatment), or injected with PTD-FNK (FNK; $n=6$), Z-VAD-FMK (VAD; $n=6$) or a combination of PTD-FNK and Z-VAD-FMK (FNK + VAD; $n=6$) 30 min after the administration of CCl_4 (post-treatment). After 20 h, serum (a) ALT and (b) AST activities were examined and the mean is shown with the S.D. (vertical bars). Statistical analysis was performed using one-way ANOVA. (c–f) H&E-stained liver tissue sections in the acute phase. Animals pre-injected with (c) vehicle or (d) PTD-FNK (300 $\mu\text{g/kg}$), or post-injected with (e) PTD-FNK or (f) a combination of PTD-FNK and Z-VAD-FMK, were treated with CCl_4 . After 20 h, animals were transcardially perfused with 4% paraformaldehyde to prepare paraffin sections of the liver, which were stained with H&E. Scale bar; 100 μm

Thus, post-injection of PTD-FNK with Z-VAD-FMK greatly exhibited the protective effect for acute CCl_4 -induced liver injury to the same extent as pre-injection of PTD-FNK.

PTD-FNK prevents chronic liver injury caused by CCl_4

For chronic liver injury, mice were given CCl_4 twice a week for 1 month. On day 4 after the final administration, livers were

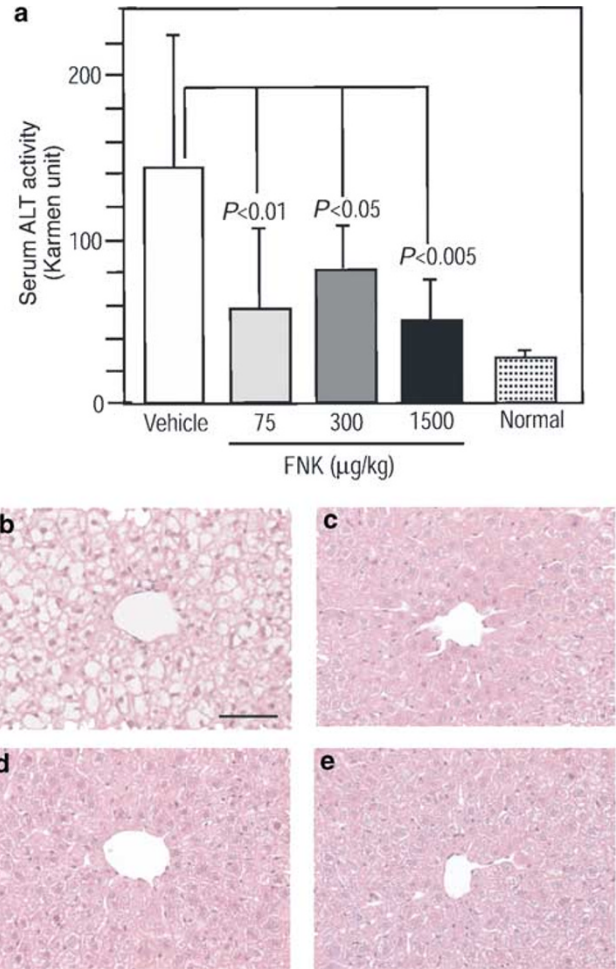


Figure 7 PTD-FNK prevents chronic liver injury caused by CCl_4 . (a) Animals were *s.c.* injected with vehicle ($n=6$) or PTD-FNK (FNK; 75 $\mu\text{g/kg}$, $n=5$; 300 $\mu\text{g/kg}$, $n=6$; 1500 $\mu\text{g/kg}$, $n=6$) 3 h before the subcutaneous injection of CCl_4 , twice a week for a month. On the 4th day after the final administration, serum ALT activity was examined. Normal mice (Normal; $n=6$) without any treatment were also examined. The mean is shown with the S.D. (vertical bars). Statistical analysis was performed using one-way ANOVA. (b–e) H&E-stained liver tissue sections in the chronic phase. Animals described in (a) were sacrificed on the 4th day after the final administration. Livers were taken out to be fixed with 4% paraformaldehyde and embedded in paraffin. The paraffin sections were stained with H&E. (b) vehicle, (c) 75 $\mu\text{g/kg}$, (d) 300 $\mu\text{g/kg}$ and (e) 1500 $\mu\text{g/kg}$. Scale bar; 100 μm

histopathologically examined and the ALT activity in serum was measured. Histopathological analysis showed that subcutaneous injection of PTD-FNK (75–1500 $\mu\text{g/kg}$) exhibited marked protective effects on the toxic changes caused by CCl_4 , compared with control mice (Table 1). The serum ALT activity of vehicle-injected mice was five to six times higher than the normal level (normal mice without any treatment) (Figure 7a). In mice injected with PTD-FNK, at 75–1500 $\mu\text{g/kg}$, the activity of serum ALT was markedly lower than that in vehicle-injected mice. Zonal necrosis in the liver of PTD-FNK-treated mice was clearly reduced (Figure 7b–e and Table 1). Taken together, PTD-FNK mitigated chronic liver injury caused by CCl_4 .

Table 1 Histopathological analysis of CCl₄-induced liver injury by a semi-quantitative procedure

	PTD-FNK ($\mu\text{g}/\text{kg}$)	Animal no.	Zonal necrosis				Cytoplasm				Nucleus							
			-	+	++	+++	Hydropic degeneration				Pyknosis				Loss			
							-	+	++	+++	-	+	++	+++	-	+	++	+++
Acute	0	4	0	0	0	4	0	0	0	4	0	0	0	4	0	0	4	0
	300 (pre)	4	4	0	0	0	0	0	4	0	0	0	4	0	2	2	0	0
	300 (post)	6	4	2	0	0	0	0	6	0	0	4	2	0	4	2	0	0
	300 with VAD (post)	6	5	1	0	0	0	5	1	0	0	4	2	0	0	6	0	0
Chronic	0	6	0	0	2	4	0	0	2	4	0	0	0	6	0	0	0	6
	75	5	0	2	3	0	0	0	5	0	0	0	5	0	0	4	1	0
	300	6	0	3	3	0	0	0	6	0	0	0	6	0	0	4	2	0
	1500	6	0	3	3	0	0	0	6	0	0	1	5	0	0	5	1	0

–, no pathological findings; +, mild; ++, moderate; +++, severe

PTD-FNK also prevents liver injury induced by ethanol and dexamethasone (DEX)

Next, we examined whether PTD-FNK is applicable to the other models of hepatic injury. EtOH was injected to generate an experimental model of alcoholic hepatic injury. In fact, it caused many lipid deposits (fatty degeneration) to form in the cytoplasm of hepatic cells and also pyknosis in some cells at 12 h (Figure 8a). Injection of PTD-FNK (20 mg/kg, *i.p.*) inhibited the nuclear degeneration but not the fatty degeneration (Figure 8b and Table 2).

A synthetic soluble glucocorticoid, DEX, is an anti-inflammatory drug but affects some hepatotoxicity.⁴⁴ The adverse effect by DEX on the liver was evident (Figure 8c). The DEX treatment markedly resulted in the loss of the eosinophilic compartment from the cytoplasm of hepatic cells, which appeared to represent zonal necrosis, but no cholestasis was observed (Figure 8c). Injection of PTD-FNK (5 mg/kg, *i.p.*) clearly ameliorated the zonal necrosis (Figure 8d) and cytoplasmic and nuclear degeneration (Table 2). As DEX induces apoptosis at high doses, liver sections were stained using the TUNEL assay. In vehicle-injected liver sections, DEX induced many TUNEL-positive cells (Figure 8e), while PTD-FNK reduced the number of TUNEL-positive cells by half, indicating that PTD-FNK prevents DEX-induced hepatic injury. Thus, PTD-FNK seemed to protect hepatocytes against various injuries regardless of apoptosis or necrosis.

Discussion

We addressed the question of whether FNK can protect cells from necrotic death via protein transduction technology using the PTD of HIV/Tat.

Under *in vitro* experimental conditions, the addition of 80%-saturated CCl₄/DMEM lacking serum caused death of HepG2 cells with no activation of caspase-3/caspase-3-like activity, no nuclear fragmentation, no ladder formation of DNA in 8 h, and no binding to Annexin V in the early stage. Detection of a 50 kDa fragment derived from PARP-1 in CCl₄-treated cells is strong evidence for necrosis, because the apoptotic PARP-1 fragment of 85 kDa induced with TNF α /CHX is distinct from the 50 kDa fragment^{38,39} (Figure 1d). These results clearly

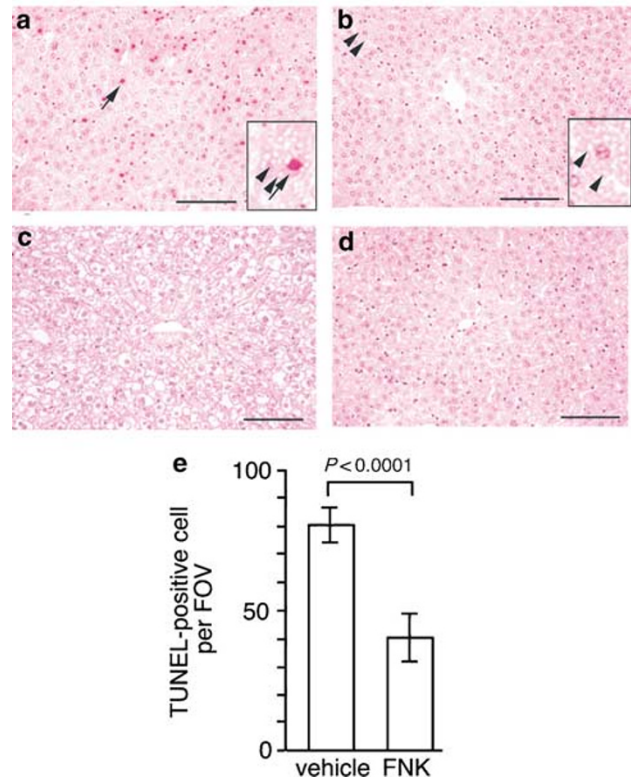


Figure 8 PTD-FNK prevents liver injury induced by ethanol or dexamethasone. Mice were intraperitoneally injected with vehicle or PTD-FNK 3 h before the administration of drugs. (a and b) Ethanol-induced injury. Mice pre-injected with vehicle (a) or PTD-FNK (20 mg/kg) (b) were treated with ethanol. After 12 h, animals were transcardially perfused and liver sections were stained with H&E. Arrows and arrowheads indicate pyknosis and lipid deposits, respectively, and have been enlarged in the insets. (c and d) DEX-induced injury. Mice pre-injected with vehicle (c) and PTD-FNK (5 mg/kg) (d) were treated with DEX. After 24 h, animals were transcardially perfused and liver sections were stained with H&E. Scale bars: (a–d), 100 μm . (e) The number of TUNEL-positive cells per high-powered field of view (FOV) in the liver sections prepared from the DEX-treated mice injected with vehicle or PTD-FNK (FNK). TUNEL-positive cells were counted in five non-overlapping fields per slide from each liver ($n=20$ microscopic fields). The vertical bars show the S.D. and statistical analysis was performed using the Student's *t*-test

Table 2 Histopathological analysis of ethanol (EtOH)- or dexamethasone (DEX)-induced liver injury by a semi-quantitative procedure

PTD-FNK (mg/kg)	Animal no.	Zonal necrosis				Cytoplasm								Nucleus									
		-	+	++	+++	Hydropic degeneration				Fatty degeneration				Pyknosis				Loss					
						-	+	++	+++	-	+	++	+++	-	+	++	+++	-	+	++	+++		
EtOH	0	4	4	0	0	0	4	0	0	0	0	0	4	0	0	4	0	0	0	4	0	0	0
	20	4	4	0	0	0	4	0	0	0	0	0	4	0	0	4	0	0	0	4	0	0	0
DEX	0	4	0	0	0	4	0	0	1	3	4	0	0	0	0	0	1	3	0	0	4	0	0
	5	4	0	4	0	0	0	0	4	0	4	0	0	0	2	2	0	0	4	0	0	0	0

-, no pathological findings; +, mild; ++, moderate; +++, severe

indicated that a majority of HepG2 cells exposed to CCl₄ died in a necrotic manner, with a good agreement with previous results.⁴⁵ The results of the application of PTD-FNK and PTD-Bcl-x_L have two implications. The first is that PTD-FNK significantly protected the cells from necrotic death induced by CCl₄, compared with PTD-Bcl-x_L. The second is that PTD-FNK clearly increased the apoptotic population among cells treated with CCl₄. The result may imply that the necrotic pathway activated by CCl₄ uses apoptotic mediator(s) in some steps, as discussed below. In fact, PTD-FNK with Z-VAD-FMK protected around 60% of cells from CCl₄-induced necrotic death. A plausible explanation for these results is that treatment with PTD-FNK or -Bcl-x_L caused a switch from a necrotic to apoptotic pathway and that, in turn, Z-VAD-FMK protects these cells from the apoptosis. On the other hand, a small population among the HepG2 cells treated with CCl₄ had fragmented nuclei even in the absence of PTD-FNK (Figure 3a). However, the apoptotic morphology seems to be caused by the withdrawal of serum but not by the addition of CCl₄ because the Annexin-V-positive and PI-negative population was equivalent between cells treated and untreated with CCl₄ (Figure 3d). In double-positive cells with Annexin V and PI, Annexin V may have entered into cells and bound to phosphatidylserine remaining at inner side of the plasma membrane.⁴⁶

Apoptosis has been distinguished from necrosis by morphological and biochemical characteristics including activation of caspases. Recent evidences showed that some biochemical and morphological characteristics of both modes of cell death can be found in the same cell.¹ It is also argued that physiological cell deaths exist that do not appear to be typical apoptosis or dependent on the caspase activation.⁴⁷ Appearance of these complex death forms can be explained by interception of active cellular death processes by, for example, oxygen-radical scavengers and inhibition of caspase or PARP.⁴⁸⁻⁵⁰ Our results support the hypothesis that necrosis and typical apoptosis are two extremes of a spectrum of death programs varying with the strength of the death stimulus.¹ It is noted that mitochondria play an important role in necrosis as well as apoptosis.^{1,47} As PTD-FNK was shown to localize in the mitochondria,^{17,18} further studies on the function of PTD-FNK would provide insight into the correlation between apoptosis and necrosis. Since FNK exhibited clearer results than Bcl-x_L, FNK will be useful for investigating this issue in future.

How does PTD-FNK protect cells from CCl₄-induced necrosis? The hepatic cell death caused by CCl₄ is clearly due to necrosis (oncosis), although a careful study demonstrated that a small population of hepatocytes undergoes apoptosis in acute CCl₄-induced liver injury.⁵¹ It is generally accepted that CCl₄ is metabolized to the trichloromethyl free radical by the monooxidase system of the ER, where cytochrome P450, mainly isozyme CYP2E1, is thought to play an important role in the pathogenesis.⁵² Following production of toxic reactive intermediates, autocatalytic lipid peroxidation is suggested to damage cellular macromolecules, but the cellular mechanisms responsible for CCl₄-induced hepatic cell death are poorly understood.⁵³ The HepG2 cells used here do not express significant amounts of the enzyme.⁵⁴ Since PTD-FNK retained the intracellular level of ATP and mitochondrial membrane potential, the protein seems to preserve functional mitochondria to protect cells.

Another evidence is emerging that calcium ions are involved in the CCl₄-induced cytotoxicity.⁵³⁻⁵⁶ CCl₄ affects intracellular Ca²⁺ content and seems to inhibit differently calcium transport systems on the cytoplasmic, mitochondrial and ER membranes.⁵⁶ Calcium ions activate lytic enzymes such as phospholipase A2 that may cause disintegrity of the organelle membrane, including the cytoplasmic membrane.⁵⁷ Thus, cytoplasmic Ca²⁺ seems generally to play a key role in necrosis. Interestingly, many studies indicate alterations in the intracellular Ca²⁺ homeostasis to control apoptosis.⁵⁸ Bcl-2 inhibits a release of Ca²⁺ from the ER induced by the pro-apoptotic Bcl-2 family members Bax or Bak.⁵⁹ PTD-FNK likely inhibits the disruption of Ca²⁺ homeostasis induced by CCl₄ because PTD-FNK affects the cytosolic movement of Ca²⁺ and protects neuronal cells from glutamate excitotoxicity.¹⁸

PTD-FNK injected into mice was successfully delivered to the liver and prevented the acute and chronic death of hepatocytes caused by CCl₄. On post-injection of PTD-FNK, an injection of Z-VAD-FMK significantly reduced the acute liver injury, as expected from the *in vitro* studies, indicating that the therapeutic window for combined injections extends after the administration of CCl₄. PTD-FNK injection also prevented alcohol- and DEX-induced liver injury. Ethanol was recently shown to generate free radicals in mice and rats,^{60,61} increasing the frequency of DNA-strand breaks in the liver.⁶⁰ PTD-FNK probably inhibited pyknosis caused by free radicals, while it did not affect fatty accumulation as a

product of the EtOH metabolism. DEX treatment decreases the glutathione concentration in liver⁴⁴ and, at a high dose, causes reversible hepatomegaly with hepatopathy.⁶² It is also reported that DEX co-administered with methotrexate induced liver damage during a treatment for brain tumor.⁶³

This study strongly suggests that PTD-FNK is a potent therapeutic protein to prevent necrotic and apoptotic cell death for emergency care and will allow the development of a novel therapy to prevent cell death by preventing necrosis.

Materials and Methods

Preparation of PTD-FNK

PTD-FNK and PTD-Bcl-x_L were prepared as described previously.¹⁸ In brief, the proteins were recovered as inclusion bodies from *Escherichia coli* cells after treatment with isopropyl 1-thio-β-D-galactoside. The proteins were solubilized in a buffer (7 M urea, 2% SDS, 1 mM DTT, 62.5 mM Tris-HCl (pH 6.8) and 150 mM NaCl), and then subjected to SDS-PAGE to remove contaminating proteins and endotoxin. The gel was treated with 1 M KCl and the transparent band corresponding to PTD-FNK or PTD-Bcl-x_L was cut out. The proteins were electrophoretically extracted from the gel slice in an extraction buffer (25 mM Tris, 0.2 M glycine and 0.1% SDS) for *in vitro* and *in vivo* experiments. The extraction buffer was used as a control (vehicle). The concentration of PTD-FNK or PTD-Bcl-x_L extracted ranged from 1 to 2.5 mg/ml.

Chemicals

CCl₄ and STS were purchased from Wako Pure Chemical Industries Ltd (Osaka, Japan) and Sigma (Sigma-Aldrich Japan, Tokyo, Japan), respectively. Caspase inhibitor I, Z-VAD-FMK, was obtained from Calbiochem (Merck Japan Ltd, Tokyo, Japan). Human recombinant TNFα was purchased from Sigma. Olive oil (Sigma) was used as a solvent of CCl₄ for injection.

Cell culture and drug-inducing cell death

The human hepatoma cell line HepG2 was cultured in DMEM (Life Technologies, Invitrogen, Tokyo, Japan) containing 10% fetal bovine serum (FBS). Cells were plated at 5×10^3 (or 1×10^4) cells/well in a 48-well (or 24-well) IWAKI EZView™ culture plate (Asahi Techno Glass, Tokyo, Japan), which had been coated with collagen type I (Cellmatrix I-P, Nitta Gelatin Inc., Osaka, Japan). After 2 days, the cells were treated with drugs. For CCl₄ treatment, cells were washed with FBS-free DMEM twice and treated with 80%-saturated CCl₄ in DMEM without FBS. FBS-free DMEM was brought to 80% CCl₄ saturation by adding CCl₄-saturated DMEM, where the CCl₄-saturated DMEM was prepared as follows: excess amounts of CCl₄ were added to FBS-free DMEM in a glass bottle and incubated for 15–18 h at 37°C. Hoechst 33342 and PI, 5 μM each, were added to the cells after various incubation periods. To detect cells in the early stage of apoptosis, the cells were stained with Annexin-V-FLUOS (green dye) and PI using a Annexin-V-FLUOS Staining Kit (Roche Diagnostics GmbH, Mannheim, Germany). Annexin-V-positive and PI-negative cells were judged as apoptotic ones. For STS treatment, cells in DMEM with FBS were treated with 10 μM STS. For TNFα treatment, cells in DMEM with FBS were pretreated with CHX (10 μg/ml) for 30 min, and then TNFα was added at the concentration of 1 and 10 ng/ml.

Caspase-3/caspase-3-like activity assay and DNA fragmentation

HepG2 (1×10^5) cells were plated in a 60-mm glass dish coated with collagen type I. After 2 days, the cells were treated with CCl₄ or STS for various periods as mentioned above. Harvested cells were lysed and a caspase fluorescence assay was performed using Ac-DEVD-AMC (N-acetyl-Asp-Glu-Val-Asp-7-amino-4-methylcoumarin), with or without the inhibitor Ac-DEVD-CHO (N-acetyl-Asp-Glu-Val-Asp-CHO (aldehyde)), and a Caspase Fluorescent (AMC) Substrate/Inhibitor QuantiPack™ (BIOMOL Research Laboratories Inc., PA, USA). Protein concentration was determined with the BCA Protein Assay (Pierce, IL, USA) using BSA as a standard. For the detection of DNA ladders, harvested cells were lysed with 0.5% Triton X-100, and then centrifuged to remove intact nuclei as reported previously.⁶⁴ After digestion with proteinase K and RNase A, fragmented DNA was precipitated with 2-propanol. DNA from 0.6×10^5 cells was subjected to electrophoresis on a 2% agarose gel, stained with SYBR Green (Molecular Probes Inc., OR, USA). With this method, DNA from intact nuclei was excluded, and thus the intact DNA did not disturb the pattern of electrophoresis.

Western blot analysis

Cells were harvested and washed. The total protein was solubilized in the presence of 2% SDS by sonication. Protein concentration was determined with the BCA Protein Assay (Pierce) using BSA as a standard. After separated on a SDS-polyacrylamide gradient (4–20%) gel, the proteins were transferred onto a PolyScreen polyvinylidene fluoride membrane (NEN Life Science Product Inc., Boston, MA, USA). The membrane was treated with anti-human PARP (clone 7D3-6; BD Biosciences Pharmingen, San Diego CA, USA). The intact form and digested products of PARP-1 were visualized with a fluoro bioimaging analyzer FLA-2000 (Fuji Photo Film, Tokyo) using the AttoPhos kit (Roche Diagnostics K.K., Tokyo).

ATP measurement

Cells were plated at 5×10^3 cells/well in a 48-well IWAKI EZView™ culture plate coated with collagen type I. After 2 days, the cells were treated with 80%-saturated CCl₄/DMEM for 0 to 4 h. After the CCl₄/DMEM solution was removed, 100 μl of DMEM without FBS was added to the wells and ATP levels were determined using a 'Cellno' ATP Assay Kit Type N (TOYO B-Net Co., Ltd, Tokyo) as per the manufacturer's instructions. Briefly, 100 μl of the lysis/assay solution provided by the manufacturer was added to the wells. After shaking for 1 min and incubating for 10 min at 23°C, luminescence of an aliquot of the solution was measured in a luminometer, Lumat LB9507 (Berthold Technologies, Berthold Japan Co., Ltd, Tokyo).

Membrane potential measurement

Cells were plated at 1×10^4 cells/well in a 24-well IWAKI EZView™ culture plate coated with collagen type I. After 2 days, the cells were treated with 80%-saturated CCl₄/DMEM for 0 and 4 h. The CCl₄ solution was removed and DMEM containing 100 nM MitoTracker Red CMXRos (Molecular Probes) and 200 nM MitoTracker Green FM (Molecular Probes) was added. After 30-min incubation, fluorescence was imaged by confocal scanning laser microscopy (Fluoview FV300; Olympus, Tokyo). The images were analyzed by using the NIH IMAGE program to obtain a ratio of mean intensity in red divided by mean intensity in green of each cell, where the ratio reflects mitochondrial membrane potential of each cell.

Drug-induced liver injury

Male, 4- to 5-week-old C57BL/6N mice (Seac Yoshitomi Ltd, Yoshitomi-cho, Fukuoka, Japan) were used. For acute liver injury induced by CCl₄, mice were *i.p.* injected with CCl₄ (25 mg/kg). After 20 h, blood was obtained for biochemical examinations and mice were perfused transcidentally and livers fixed with 4% paraformaldehyde in 0.1 M phosphate buffer (pH 7.4), dehydrated and embedded in paraffin. For acute liver injury induced by ethanol and DEX (Sigma), ethanol (5 g/kg) or DEX (25 mg/kg) was *i.p.* administered. After specified periods, mice were transcidentally perfused and livers fixed with 4% paraformaldehyde, dehydrated and embedded in paraffin as described above. For chronic liver injury caused by CCl₄, mice were subcutaneously injected with vehicle or PTD-FNK 3 h before the subcutaneous injection of CCl₄ (25 mg/kg), twice a week for a month. On the 4th day after the final administration, blood was obtained for biochemical examinations and mice were killed. Livers were removed for fixation with 4% paraformaldehyde in 0.1 M phosphate buffer (pH 7.4), dehydrated and embedded in paraffin. Tissues were sectioned (4 μm), and stained with H&E for histopathological analysis. Activities of serum AST and ALT were evaluated using a Transaminase CII Testwako kit (Wako Pure Chemical Industries Ltd). Animal protocols were approved by the Animal Care and Use Committee of Nippon Medical School.

Immunohistochemical staining

The delivery of PTD-FNK into the liver was examined according to the manufacturer's protocol using a Vectastain ABC elite kit (Vector Laboratories, Burlingame, CA, USA) coupled to a diaminobenzidine (DAB) reaction. Rabbit polyclonal anti rat Bcl-x serum (diluted 1:250 at 4°C overnight) was used as a primary antibody. In addition, phosphate-buffered saline (PBS) was utilized instead of primary antibody and/or ABC reagent as a negative control.

Terminal deoxynucleotidyl transferase-mediated dUTP nick-end labeling (TUNEL)

Separate sections were used for TUNEL staining using an ApopTag peroxidase *In situ* Apoptosis Detection Kit (Intergen Company, Purchase, New York, USA), and visualized with DAB. For negative controls, terminal deoxynucleotidyl transferase was omitted. In each section, TUNEL-positive cells were counted in five non-overlapping microscopic fields (× 100 magnification).

References

- Proskuryakov SY, Konoplyannikov AG and Gabai VL (2003) Necrosis: a specific form of programmed cell death? *Exp. Cell Res.* 283: 1–16
- Nathan C (2002) Points of control in inflammation. *Nature* 420: 846–852
- Roos KL (1990) Dexamethasone and nonsteroidal anti-inflammatory agents in the treatment of bacterial meningitis. *Clin. Ther.* 12: 290–296
- Tracey KJ (2002) The inflammatory reflex. *Nature* 420: 853–859
- Palladino MA, Bahjat FR, Theodorakis EA and Moldawer LL (2003) Anti-TNF-α therapies: the next generation. *Nat. Rev. Drug Discov.* 2: 736–746
- Boise LH, Gonzalez-Garcia M, Postema CE, Ding L, Lindsten T, Turka LA, Mao X, Nunez G and Thompson CB (1993) *bcl-x*, a *bcl-2*-related gene that functions as a dominant regulator of apoptotic cell death. *Cell* 74: 597–608
- Minn AJ, Rudin CM, Boise LH and Thompson CB (1995) Expression of Bcl-x_L can confer a multidrug resistance phenotype. *Blood* 86: 1903–1910
- Yang J, Liu X, Bhalla K, Kim CN, Ibrado AM, Cai J, Peng TI, Jones DP and Wang X (1997) Prevention of apoptosis by Bcl-2: release of cytochrome c from mitochondria blocked. *Science* 275: 1129–1132
- Jäättelä M, Benedict M, Tewari M, Shayman JA and Dixit VM (1995) Bcl-x and Bcl-2 inhibit TNF and Fas-induced apoptosis and activation of phospholipase A2 in breast carcinoma cells. *Oncogene* 10: 2297–2305
- Fukunaga-Johnson N, Ryan JJ, Wicha M, Nunez G and Clarke MF (1995) Bcl-2 protects murine erythroleukemia cells from p53-dependent and -independent radiation-induced cell death. *Carcinogenesis* 16: 1761–1767
- Cory S, Huang DC and Adams JM (2003) The Bcl-2 family: roles in cell survival and oncogenesis. *Oncogene* 22: 8590–8607
- Tsujimoto Y, Shimizu S, Eguchi Y, Kamiike W and Matsuda H (1997) Bcl-2 and Bcl-x_L block apoptosis as well as necrosis: possible involvement of common mediators in apoptotic and necrotic signal transduction pathways. *Leukemia* 11: 380–382
- Single B, Leist M and Nicotera P (2001) Differential effects of *bcl-2* on cell death triggered under ATP-depleting conditions. *Exp. Cell Res.* 262: 8–16
- Asoh S, Ohtsu T and Ohta S (2000) The super anti-apoptotic factor Bcl-x_{FM} constructed by disturbing intramolecular polar interactions in rat Bcl-x_L. *J. Biol. Chem.* 275: 37240–37245
- Nagahara H, Vocero-Akbani AM, Snyder EL, Ho A, Latham DG, Lissy NA, Becker-Hapak M, Ezhevsky SA and Dowdy SF (1998) Transduction of full-length TAT fusion proteins into mammalian cells: TAT-p27^{Kip1} induces cell migration. *Nat. Med.* 4: 1449–1452
- Schwarze SR, Ho A, Vocero-Akbani A and Dowdy SF (1999) *In vivo* protein transduction: delivery of a biologically active protein into the mouse. *Science* 285: 1569–1572
- Ozaki D, Sudo K, Asoh S, Yamagata K, Ito H and Ohta S (2004) Transduction of anti-apoptotic proteins into chondrocytes in cartilage slice culture. *Biochem. Biophys. Res. Commun.* 313: 522–527
- Asoh S, Ohsawa I, Mori T, Katsura K, Hiraide T, Katayama Y, Kimura M, Ozaki D, Yamagata K and Ohta S (2002) Protection against ischemic brain injury by protein therapeutics. *Proc. Natl. Acad. Sci. USA* 99: 17107–17112
- Graham SH and Chen J (2001) Programmed cell death in cerebral ischemia. *J. Cereb. Blood Flow Metab.* 21: 99–109
- Valencia A and Moran J (2004) Reactive oxygen species induce different cell death mechanisms in cultured neurons. *Free Radic. Biol. Med.* 36: 1112–1125
- Lin Y, Choksi S, Shen HM, Yang QF, Hur GM, Kim YS, Tran JH, Nedospasov SA and Liu ZG (2004) Tumor necrosis factor-induced nonapoptotic cell death requires receptor-interacting protein-mediated cellular reactive oxygen species accumulation. *J. Biol. Chem.* 279: 10822–10828
- Higuchi M, Honda T, Proske RJ and Yeh ET (1998) Regulation of reactive oxygen species-induced apoptosis and necrosis by caspase 3-like proteases. *Oncogene* 17: 2753–2760
- Lee WT, Itoh T and Pleasure D (2002) Acute and chronic alterations in calcium homeostasis in 3-nitropropionic acid-treated human NT2-N neurons. *Neuroscience* 113: 699–708
- Zhu LP, Yu XD, Ling S, Brown RA and Kuo TH (2000) Mitochondrial Ca²⁺ homeostasis in the regulation of apoptotic and necrotic cell deaths. *Cell Calcium* 28: 107–117
- Gwag BJ, Canzoniero LM, Sensi SL, Demaro JA, Koh JY, Goldberg MP, Jacquin M and Choi DW (1999) Calcium ionophores can induce either apoptosis or necrosis in cultured cortical neurons. *Neuroscience* 90: 1339–1348
- Pritchard DJ and Butler WH (1989) Apoptosis – the mechanism of cell death in dimethylnitrosamine-induced hepatotoxicity. *J. Pathol.* 158: 253–260
- Fukuda K, Kojiro M and Chiu JF (1993) Demonstration of extensive chromatin cleavage in transplanted Morris hepatoma 7777 tissue: apoptosis or necrosis? *Am. J. Pathol.* 142: 935–946
- Grasl-Kraupp B, Ruttkay-Nedecky B, Koudelka H, Bukowska K, Bursch W and Schulte-Hermann R (1995) *In situ* detection of fragmented DNA (TUNEL assay) fails to discriminate among apoptosis, necrosis, and autolytic cell death: a cautionary note. *Hepatology* 21: 1465–1468
- Columbano A, Endoh T, Denda A, Noguchi O, Nakae D, Hasegawa K, Ledda-Columbano GM, Zedda AI and Konishi Y (1996) Effects of cell proliferation and cell death (apoptosis and necrosis) on the early stages of rat hepatocarcinogenesis. *Carcinogenesis* 17: 395–400
- Noguchi T, Fong KL, Lai EK, Alexander SS, King MM, Olson L, Poyer JL and McCay PB (1982) Specificity of a phenobarbital-induced cytochrome P-450 for

- metabolism of carbon tetrachloride to the trichloromethyl radical. *Biochem. Pharmacol.* 31: 615–624
31. Ahr HJ, King LJ, Nastainczyk W and Ullrich V (1982) The mechanism of reductive dehalogenation of halothane by liver cytochrome P450. *Biochem. Pharmacol.* 31: 383–390
 32. Nastainczyk W, Ahr HJ and Ullrich V (1982) The reductive metabolism of halogenated alkanes by liver microsomal cytochrome P450. *Biochem. Pharmacol.* 31: 391–396
 33. Poyer JL, McCay PB, Lai EK, Janzen EG and Davis ER (1980) Confirmation of assignment of the trichloromethyl radical spin adduct detected by spin trapping during ^{13}C -carbon tetrachloride metabolism *in vitro* and *in vivo*. *Biochem. Biophys. Res. Commun.* 94: 1154–1160
 34. Lai EK, McCay PB, Noguchi T and Fong KL (1979) *In vivo* spin-trapping of trichloromethyl radicals formed from CCl_4 . *Biochem. Pharmacol.* 28: 2231–2235
 35. Berger ML, Bhatt H, Combes B and Estabrook RW (1986) CCl_4 -induced toxicity in isolated hepatocytes: the importance of direct solvent injury. *Hepatology* 6: 36–45
 36. Jones BE, Lo CR, Liu H, Srinivasan A, Streetz K, Valentino KL and Czaja MJ (2000) Hepatocytes sensitized to tumor necrosis factor- α cytotoxicity undergo apoptosis through caspase-dependent and caspase-independent pathways. *J. Biol. Chem.* 275: 705–712
 37. Bai J and Cederbaum AI (2000) Overexpression of catalase in the mitochondrial or cytosolic compartment increases sensitivity of HepG2 cells to tumor necrosis factor- α -induced apoptosis. *J. Biol. Chem.* 275: 19241–19249
 38. Gobeil S, Boucher CC, Nadeau D and Poirier GG (2001) Characterization of the necrotic cleavage of poly(ADP-ribose) polymerase (PARP-1): implication of lysosomal proteases. *Cell Death Differ.* 8: 588–594
 39. Shah GM, Shah RG and Poirier GG (1996) Different cleavage pattern for poly(ADP-ribose) polymerase during necrosis and apoptosis in HL-60 cells. *Biochem. Biophys. Res. Commun.* 229: 838–844
 40. Aikin R, Rosenberg L, Paraskevas S and Maysinger D (2004) Inhibition of caspase-mediated PARP-1 cleavage results in increased necrosis in isolated islets of Langerhans. *J. Mol. Med.* 82: 389–397
 41. Horn TL, O'Brien TD, Schook LB and Rutherford MS (2000) Acute hepatotoxicant exposure induces TNFR-mediated hepatic injury and cytokine/apoptotic gene expression. *Toxicol. Sci.* 54: 262–273
 42. Morio LA, Chiu H, Sprowles KA, Zhou P, Heck DE, Gordon MK and Laskin DL (2001) Distinct roles of tumor necrosis factor- α and nitric oxide in acute liver injury induced by carbon tetrachloride in mice. *Toxicol. Appl. Pharmacol.* 172: 44–51
 43. Simeonova PP, Gallucci RM, Hulderman T, Wilson R, Kommineni C, Rao M and Luster MI (2001) The role of tumor necrosis factor- α in liver toxicity, inflammation, and fibrosis induced by carbon tetrachloride. *Toxicol. Appl. Pharmacol.* 177: 112–120
 44. Madhu C, Maziasz T and Klaassen CD (1992) Effect of pregnenolone-16 α -carbonitrile and dexamethasone on acetaminophen-induced hepatotoxicity in mice. *Toxicol. Appl. Pharmacol.* 115: 191–198
 45. Jäättelä M and Tschopp J (2003) Caspase-independent cell death in T lymphocytes. *Nat. Immunol.* 4: 416–423
 46. Vermes I, Haanen C, Steffens-Nakken H and Reutelingsperger C (1995) A novel assay for apoptosis. Flow cytometric detection of phosphatidylserine expression on early apoptotic cells using fluorescein labelled Annexin V. *J. Immunol. Methods.* 184: 39–51
 47. Lockshin RA and Zakeri Z (2004) Caspase-independent cell death? *Oncogene* 23: 2766–2773
 48. Vercammen D, Brouckaert G, Denecker G, Van de Craen M, Declercq W, Fiers W and Vandenebee P (1998) Dual signaling of the Fas receptor: initiation of both apoptotic and necrotic cell death pathways. *J. Exp. Med.* 188: 919–930
 49. Vercammen D, Beyaert R, Denecker G, Goossens V, Van Loo G, Declercq W, Grooten J, Fiers W and Vandenebee P (1998) Inhibition of caspases increases the sensitivity of L929 cells to necrosis mediated by tumor necrosis factor. *J. Exp. Med.* 187: 1477–1485
 50. Ha HC and Snyder SH (1999) Poly(ADP-ribose) polymerase is a mediator of necrotic cell death by ATP depletion. *Proc. Natl. Acad. Sci. USA* 96: 13978–13982
 51. Shi J, Aisaki K, Ikawa Y and Wake K (1998) Evidence of hepatocyte apoptosis in rat liver after the administration of carbon tetrachloride. *Am. J. Pathol.* 153: 515–525
 52. Raucy JL, Kraner JC and Lasker JM (1993) Bioactivation of halogenated hydrocarbons by cytochrome P450E1. *Crit. Rev. Toxicol.* 23: 1–20
 53. Recknagel RO, Glende Jr EA, Dolak JA and Waller RL (1989) Mechanisms of carbon tetrachloride toxicity. *Pharmacol. Ther.* 43: 139–154
 54. Cederbaum AI, Wu D, Mari M and Bai J (2001) CYP2E1-dependent toxicity and oxidative stress in HepG2 cells. *Free Radic. Biol. Med.* 31: 1539–1543
 55. Costa AK, Schieble TM, Heffel DF and Trudell JR (1987) Toxicity of calcium ionophore A23187 in monolayers of hypoxic hepatocytes. *Toxicol. Appl. Pharmacol.* 87: 43–47
 56. Hemmings SJ, Pulga VB, Tran ST and Uwiera RR (2002) Differential inhibitory effects of carbon tetrachloride on the hepatic plasma membrane, mitochondrial and endoplasmic reticular calcium transport systems: implications to hepatotoxicity. *Cell Biochem. Funct.* 20: 47–59
 57. Glende Jr EA and Pushpendran CK (1986) Activation of phospholipase A2 by carbon tetrachloride in isolated rat hepatocytes. *Biochem. Pharmacol.* 35: 3301–3307
 58. Breckenridge DG, Germain M, Mathai JP, Nguyen M and Shore GC (2003) Regulation of apoptosis by endoplasmic reticulum pathways. *Oncogene* 22: 8608–8618
 59. Nutt LK, Pataer A, Pahler J, Fang B, Roth JA, McConkey DJ and Swisher SG (2002) Bax and Bak promote apoptosis by modulating endoplasmic reticular and mitochondrial Ca^{2+} stores. *J. Biol. Chem.* 277: 9219–9225
 60. Navasumrit P, Ward TH, Dodd NJ and O'Connor PJ (2000) Ethanol-induced free radicals and hepatic DNA strand breaks are prevented *in vivo* by antioxidants: effects of acute and chronic ethanol exposure. *Carcinogenesis* 21: 93–99
 61. Kono H, Rusyn I, Yin M, Gabele E, Yamashina S, Dikalova A, Kadiiska MB, Connor HD, Mason RP, Segal BH, Bradford BU, Holland SM and Thurman RG (2000) NADPH oxidase-derived free radicals are key oxidants in alcohol-induced liver disease. *J. Clin. Invest.* 106: 867–872
 62. Verrips A, Rotteveel JJ and Lippens R (1998) Dexamethasone-induced hepatomegaly in three children. *Pediatr. Neurol.* 19: 388–391
 63. Wolff JE, Hauch H, Kuhl J, Egeler RM and Jurgens H (1998) Dexamethasone increases hepatotoxicity of MTX in children with brain tumors. *Anticancer Res.* 18: 2895–2899
 64. Asoh S, Mori T, Hayashi J and Ohta S (1996) Expression of the apoptosis-mediator Fas is enhanced by dysfunctional mitochondria. *J. Biochem. (Tokyo)* 120: 600–607